Carbohydrate Polymers 181 (2018) 1160–1168

Contents lists available at ScienceDirect

Carbohydrate Polymers

journal homepage: www.elsevier.com/locate/carbpol

Research Paper

A novel structural fucosylated chondroitin sulfate from *Holothuria Mexicana* and its effects on growth factors binding and anticoagulation

Qinying Li[a], Chao Cai[a,b], Yaoguang Chang[c], Fuming Zhang[d], Robert J. Linhardt[d], Changhu Xue[b,c], Guoyun Li[a,b,*], Guangli Yu[a,b,*]

[a] Key Laboratory of Marine Drugs, Ministry of Education, School of Medicine and Pharmacy, Shandong Provincial Key Laboratory of Glycoscience and Glycotechnology, Ocean University of China, Qingdao 266003, China
[b] Laboratory for Marine Drugs and Bioproducts, Qingdao National Laboratory for Marine Science and Technology, Qingdao 266003, China
[c] College of Food Science and Technology, Ocean University of China, Qingdao, Shandong, 266003, China
[d] Department of Chemistry and Chemical Biology, Biomedical Engineering, Biology, Chemical and Biological Engineering, and Center for Biotechnology and Interdisciplinary Studies, Rensselaer Polytechnic Institute, Troy, NY 12180, USA

ARTICLE INFO

Keywords:
Fucosylated chondroitin sulfate
Holothuria mexicana
Structure elucidation
Anti-angiogenesis
Anticoagulant

ABSTRACT

Fucosylated chondroitin sulfate (FCS), a structurally distinct glycosaminoglycan from the body wall of sea cucumber, possesses many biological properties and pharmacology functions. The refined structure of FCS isolated from sea cucumber *Holothuria Mexicana* (FCS_{hm}) was characterized by NMR spectra and HILIC-FTMS, which demonstrated four types of branches in FCS_{hm}. Among these, two branches were α-L-Fuc-2S4S (where Fuc is fucose and S is sulfo) and α-L-Fuc-4S linked to *O*-3 of glucuronic acid residues, while others were identified as α-L-Fuc-4S and α-L-Fuc-3S4S attached to *O*-6 of *N*-acetylgalactosamine residue. Furthermore, the fucosyl branches were α-1,3-linked with different degree of polymerization from 1 to 5. FCS_{hm} exhibited high affinity to fibroblast growth factor 1 and 2, growth factors involved in neovascularization. Moreover, FCS_{hm} displayed intrinsic anticoagulant activity and inhibited thrombin and factor Xa activation by antithrombin III. Our results proposed a novel structural FCS and demonstrated its favorable application prospects in anti-angiogenesis and anticoagulation.

1. Introduction

Sea cucumbers have been used as a traditional tonic food in China and other Asian countries over many centuries. The major edible and medicinal parts of sea cucumbers are the body walls, which contain many bioactive components, such as polysaccharides, sea cucumber saponins, cerebrosides and gangliosides (Conand, 2001; Conand & Byrne, 1993; Lawrence, 2010). Acidic polysaccharides, among the most important components in sea cucumbers, are mainly divided into two types: fucosylated chondroitin sulfates (FCS) and fucans (Kariya, Watabe, Hashimoto, & Yoshida, 1990; Kariya, Watabe, Kyogashima, Ishihara, & Ishii, 1997; Vieira, Mulloy & Mourão, 1991). Polysaccharides obtained from sea cucumbers reportedly have anticancer, anticoagulant, antithrombotic, antiviral and neuroprotective effects (Mourão, Giumar Es, Mulloy, Thomas, & Gray, 1998; Mourão et al., 2001; Pomin, 2014a, 2014b; Taponbretaudière et al., 2002; Zhou, Xu & Shen, 2008).

FCS is a type of distinct sulfated glycosaminoglycan, composed of a backbone consisting of alternating β-1,4-linked D-glucuronic acid (GlcA) and β-1,3-linked *N*-acetyl-D-galactosamine (GalNAc) disaccharide units with α-L-fucose (Fuc) branches linked to the *O*-3 position of GlcA residues (Mourão et al., 1996). Moreover, special FCS structures with Fuc branches linked to the *O*-4 or *O*-6 position of GalNAc residues have been reported in recent years (Kariya et al., 1997; Ustyuzhanina et al., 2016, 2017).

Recently, most bioactivity studies of FCS have been focused on anticoagulation and antithrombosis. FCS exhibits excellent anticoagulant effects through thrombin (FIIa) and factor Xa (FXa) inhibition mediated through antithrombin III (ATIII), and it has been demonstrated that the molecular weight and the sulfation degree of an FCS greatly impacts its anticoagulant and antithrombotic activities (Liu, Hao et al., 2016; Liu, Liu et al., 2016; Mourão et al., 1996). FCS extracted from *Ludwigothurea grisea* shows excellent antithrombotic activity and it was shown that the sulfated fucose branches were essential for antithrombotic effectiveness (Mourão et al., 1998). Anticoagulant activities of FCSs with different sulfation patterns have also been

* Corresponding authors at: Key Laboratory of Marine Drugs, Ministry of Education, School of Medicine and Pharmacy, Shandong Provincial Key Laboratory of Glycoscience and Glycotechnology, Ocean University of China, Qingdao 266003, China
E-mail addresses: liguoyun@ouc.edu.cn (G. Li), glyu@ouc.edu.cn, glyu@hotmail.com (G. Yu).

https://doi.org/10.1016/j.carbpol.2017.10.100
Received 20 June 2017; Received in revised form 2 October 2017; Accepted 31 October 2017
Available online 02 November 2017
0144-8617/

investigated and it has been demonstrated the 2,4-*O*-sulfated fucose branch was the key structural feature required for anticoagulation and inhibition of thrombin, whereas the inhibitory effect on factor X, XII activation and thrombus generation was attributed to the overall structure of FCS (Chen et al., 2013).

Fibroblast growth factors (FGFs) are a family of polypeptide growth factors, which play key roles in a variety of biological processes, including embryonic development, cell growth, morphogenesis, tissue remodeling, angiogenesis, tumor growth and invasion (Katoh, 2002; Eswarakumar, Lax, & Schlessinger, 2005; Taponbretaudière et al., 2002). Genetic mutation of FGF receptors have been identified involving in tumorigenesis (Courjal et al., 1997; Deng et al., 2012; Turner et al., 2010; Weiss et al., 2010). Thus, FGFR-targeted therapeutics have gained increased attention. Surface plasmon resonance (SPR) is a powerful technique to measure the binding capacity between FCS and proteins. FCS obtained from sea cucumber, *Thelenota ananas*, has unique sulfated fucose branches linked to the chondroitin sulfate backbone that account for its anti-HIV-1 activity (Lian et al., 2013).

In this paper, a novel FCS (FCS_{hm}) from sea cucumber *Holothuria Mexicana* was isolated and characterized as a distinct chemical structure from previously reported FCSs based on nuclear magnetic resonance (NMR) spectroscopy and hydrophilic interaction liquid chromography (HILIC)-Fourier transform mass spectrometry (FTMS) combined with different degradation strategies. Mild acidic hydrolysis is a powerful method to release the fucosyl branches, while free radical depolymerization can generate various oligomers keeping the natural information. Furthermore, protein-binding properties between FCS_{hm} and FGF1 and FGF2 were evaluated. In addition, the anticoagulant activity and primary mechanism were investigated, which proposed a scientific basis for reasonable application of FCS_{hm}.

2. Materials and methods

2.1. Materials and chemicals

High performance gel permeation chromatography column (Shodex OHpak SB-804 HQ and SB-802.5 HQ) was from Showa Denko K.K, Japan. Packing materials for Q Sepharose FF column was from GE Healthcare Biosciences AB, USA. Luna HILIC chromatography column was from Phenomenex, American. ATIII, bovine FXa, human FIIa, chromogenic substrate S-2765 and S-2238 were purchased from Adhoc International Technologies Co., Ltd, Beijing, China. LMWH and HP from porcine intestinal mucosa were purchased from Sigma (St. Louis, MO). Acetonitrile and ammonium acetate were of HPLC grade (Sigma Aldrich, St. Louis, MO). All other chemicals were of analytical grade.

2.2. Extraction and purification of FCS_{hm}

Crude sea cucumber polysaccharides were extracted from the body wall of the sea cucumbers *H. mexicana* by methods reported previously (Chen et al., 2011) with some modifications. Briefly, the body wall of the sea cucumbers (100 g) was minced and defatted with acetone in a volume of 1:10. After centrifugation and drying, precipitate was redissolved in 30 vols of water, and then digested with 0.5% papain (containing 5 mM EDTA and 5 mM cysteine, pH 5.7) at 60 °C for 12 h. The crude polysaccharides were precipitated by adding four volumes of ethanol and collected by centrifugation. Then, 1 M HCl was added until a pH of 2.5 following by centrifugation to remove acidic albumen. Three volumes of ethanol containing 2 M potassium acetate were added into the supernatant and the raw polysaccharide was precipitated and collected by centrifugation. Raw polysaccharide was separated by Q-Sepharose Fast Flow anion-exchange column, and eluted with a linear gradient of 0–2.0 M NaCl. FCS fractions eluted by 1.75 M NaCl were purified on a Sephadex G-200 column with 0.1 M NH_4HCO_3. Finally, FCS fractions (FCS_{hm}) were dialyzed, concentrated and lyophilized.

2.3. Molecular weight and chemical composition analysis

Sulfate content was determined by $BaCl_2$-Gelatin method (Dodgson & Price, 1962). Purity and relative molecular weight (Mw) were determined by gel filtration columns (Shodex OHpak SB-804 HQ and SB-802.5 HQ) connected to an HPLC system. Sample was eluted at a flow rate of 0.6 mL min^{-1} using isocratic gradient of 0.1 mol L^{-1} Na_2SO_4 at 35 °C and detected by RID and Ten octagonal laser scattering instrument (Wyatt). Monosaccharide composition was determined by a 1-phenyl-3-methyl-5-pyrazolone (PMP)-High Performance Liquid Chromatography (HPLC) method (Chen et al., 2008). The disaccharide composition of backbone was determined by mild acidic hydrolysis and enzymatic degradation. Briefly, to remove the fucosyl branches, FCS_{hm} (10 mg) was dissolved in 1 mL 0.1 M H_2SO_4 and reacted at 80 °C for 1 h. $Ba(OH)_2$ was added to terminate the reaction by removing excess SO_4^{-}. Then the supernatant was passed through 3 kDa of ultrafiltration membrane, and filtrate was analyzed by HILIC-FTMS/MS using a Luna HILIC column (50 × 2.0 mm, 3 μm, Phenomenex) to clarify fucosyl branches. The interception fraction was the defucosylated FCS_{hm}, and further hydrolyzed by Chondroitin ABC lyase at 37 °C overnight with gentle agitation. The identification and quantitation of each disaccharide were performed on a Welch Ultimate XB-SAX column (4.6 mm × 250 mm, 3 μm) at 40 °C with UV detection at 232 nm. The mobile phase was a mixture of H_2O (pH = 3.5, solvent A) and 2 M NaCl (pH = 3.5, solvent B) at a flow rate of 0.6 mL/min. The gradient was programmed as 100% A in the beginning, linearly changed to 50% A in 45 min.

2.4. NMR spectroscopy analysis

FCS_{hm} (40 mg) was dissolved in 500 μL 99.9% deuterium oxide and freeze-dried three-times to replace all exchangeable protons with deuterium. Then sample was re-dissolved in 500 μL D_2O and transferred into NMR tube. 1D and 2D spectra were performed at 333 K on Bruker BioSpin GmbH 600 MHz with Topspin 2.1.6 software. Chemical shifts were displayed relative to internal 3-trimethylsilylpropane sulfonic acid (DSS) at 0.00 ppm for ^{1}H and ^{13}C.

2.5. Profiling of the oligosaccharides of FCS_{hm} generated by free radical depolymerization by hydrophilic interaction liquid chromatography-Fourier transform mass spectrometry (HILIC-FTMS)

FCS_{hm} samples were completely degraded by controlled oxidative depolymerization using hydrogen peroxide and cupric acetate. The samples (1 mg) were dissolved in 500 μL 0.1 M sodium acetate-acetic acid solution containing 0.2 mM copper (II) acetate and adjusted to pH 7.0. Then 20 μL of 30% hydrogen peroxide was added and reacted at 45 °C for 3 h. Sodium bisulfite was added to terminate the reaction by removing excess unreacted hydrogen peroxide, and then the reaction mixture was desalted by Carbograph SPE column (SUPELCO, USA). 3 CV water was used to elute salt, then degradation products were eluted by 3 CV 50% acetonitrile (containing 0.1% TFA) and lyophilized. Finally, lyophilized powder was redissolved in 40 μL of 50% acetonitrile for HILIC-FTMS analysis.

HILIC-FTMS analysis was performed on an Agilent 1290 LC UPLC system (Agilent Technologies, Wilmington, DE, USA) equipped with a LTQ ORBITRAP XL mass spectrometer (Thermo, SCIENTIFIC, USA). The FCS_{hm} oligosaccharides were separated by a Luna HILIC column (150 × 2.00 mm, 3 μm, Phenomenex) at 25 °C. The mobile phase was a mixture of 5 mM NH_4OAc/98% acetonitrile (solvent A) and 5 mM NH_4OAc/H_2O (solvent B) at a flow rate of 150 μL/min. The gradient was programmed as 92% A in the beginning, linearly changed to 60% A in 58 min. The analysis was performed in the negative ion mode using a capillary temperature of 275 °C. The spray voltage was 4.2 kV and nitrogen dry gas flowed at 40 L/min. Data acquisition and analysis were performed using Xcalibur 2.0 software and GlycReSoft 1.0 software.

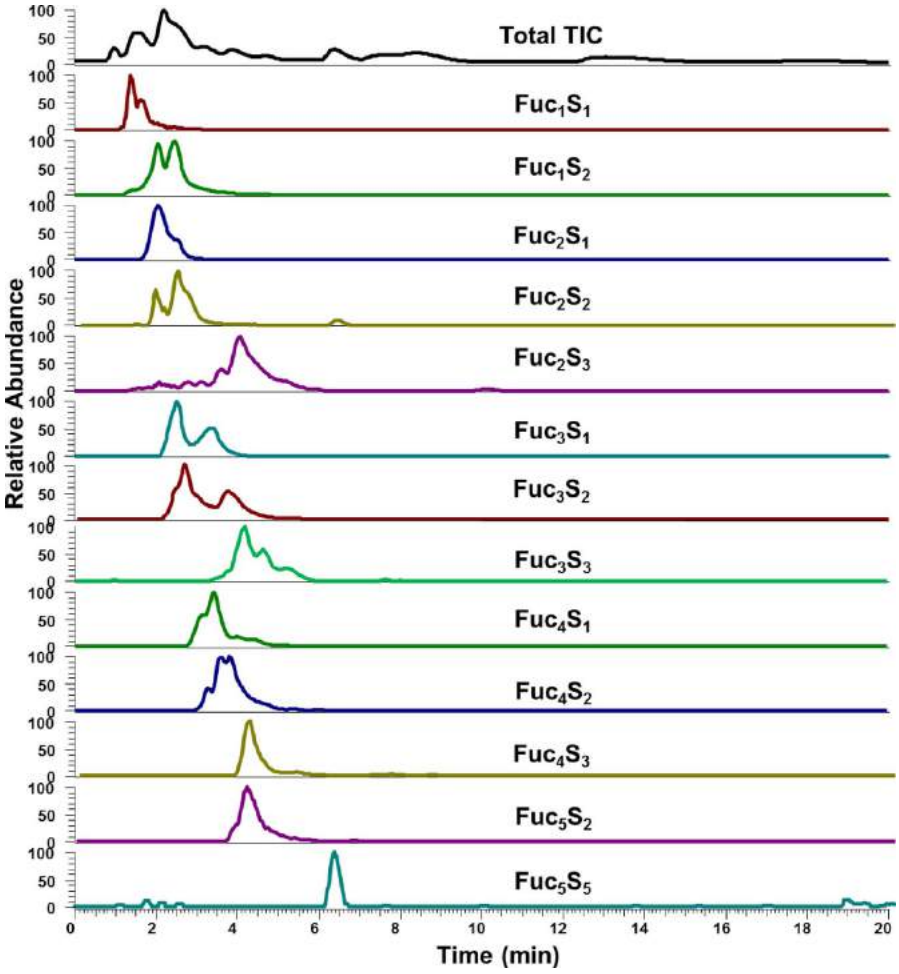

Fig. 1. Extracted ion chromatograms (EICs) of fucosyl branches based on HILIC-FTMS analysis after mild acidic hydrolysis. "Fuc" and "S" refer to fucose residue and sulfate group.

2.6. SPR binding kinetics of FGF1/FGF2-FCS$_{hm}$ interactions

SPR measurements were performed using a Biacore 3000 SPR instrument. Biotinylated FCS$_{hm}$ and FCS-*Ib* sensor chip were prepared by reaction of sulfo-N-hydroxysuccinimide long-chain biotin (Pierce, Rockford, IL) with the free amino groups and the residue with the reducing end in the polysaccharide chain following a published procedure (Weyers et al., 2013). Heparin was used as a positive control. Biotinylated polysaccharides were immobilized to streptavidin (SA) coated CM5 sensor chip (GE Healthcare, Uppsala, Sweden) using the manufacturer's protocol. In brief, 20 mL of the heparin-biotin conjugate (0.1 mg/mL) in HBS-EP (10 mM HEPES, pH 7.4, 150 mM NaCl, 3 mM EDTA, and 0.005% surfactant P20) buffer was injected over flow-cell 2, 3, 4 (FC2, 3, 4) of a SA sensor chip at a flow-rate of 10 mL/min. Approximately 100 resonance units (RU) of heparin were coupled to the sensor chip. A control flow-cell (FC) was prepared with a 1 min injection with saturated biotin in HBS-EP buffer.

The binding kinetics of the FGF1/FGF2 interactions over the polysaccharides sensor chip were assayed using HBS-EP buffer at 25 °C. Two-fold serial dilutions of FGF1/FGF2 were injected over the sensor chip at a flow-rate of 30 mL/min for a period of 3 min followed by 3 min dissociation period. The sensor chip was regenerated for subsequent runs using 30 mL injection of 2 M NaCl. SPR experiments were performed in duplicate or triplicate at each concentration, confirming reproducibility. The binding sensor grams (RU versus time) were pooled, trimmed, double referenced, and experimental fit to different kinetic models using BIAevaluation software v4.0.1.

2.7. Anticoagulant assays

Sheep plasma was purchased from Cangshan, Shandong. activated partial thromboplastin time (APTT), thrombin time (TT) and prothrombin time (PT) were measured using kits purchased from Nanjing Jiancheng Bioengineering Institute (Jiangsu, China) and a blood coagulation analyzer (SL-318, Senlan Medical Science and Trading Co., Ltd, Jinan, China).

2.8. Anti-FXa and anti-FIIa activity in the presence of ATIII

The anti-FXa and anti-FIIa activities of FCS$_{hm}$ in the presence of ATIII were estimated by published methods (Pomin, 2014a, 2014b). Incubations were performed in 96-well plates and a mixture containing 20 μL sample and 20 μL of 0.5 IU/mL ATIII was incubated at 37 °C for 2 min. Then, 40 μL of 0.25 IU/mL FXa or 5 IU/mL FIIa was added. After incubation for 1 min, the residual FXa or FIIa activity was measured by the addition of 50 μL of 1 mM FXa chromogenic substrate S-2765 or FIIa chromogenic substrate S-2238. The reaction was terminated by adding 30% of acetic acid and absorbance of the reaction mixture was recorded at 405 nm.

3. Results and discussion

Fucosylated chondroitin sulfate (FCS_{hm}) was extracted and purified from sea cucumber *Holothuria Mexicana*. Then FCS_{hm} was characterized by NMR spectroscopy and HILIC-FTMS combined with different degradation strategies. Furthermore, the protein-binding properties with FGF and anticoagulant activity of FCS_{hm} were investigated, which proposed a scientific basis for reasonable application. The flow chart of experiment was listed in Fig. S1.

3.1. Chemical composition analysis

In this study, FCS isolated from sea cucumber *H. Mexicana* was purified by Q Sepharose FF anion exchange column and Sephadex G-200 column. The physicochemical properties of FCS_{hm} were listed in Table S1. Single and symmetric peaks on both RID and laser signals indicated that FCS_{hm} was of high purity (Fig. S2). GPC analysis showed that molecular weight of FCS_{hm} from *H. mexicana* was much larger than previously reported FCSs (Liu, Hao et al., 2016; Liu, Liu et al., 2016; Wu et al., 2013). Based on Mw and radius of gyration ($< S^2 >_z^{1/2}$), we verified FCS_{hm} was highly branched macromolecules (Fig. S3) (Hu, Huang, Wong, & Yang, 2017). Monosaccharide composition analysis demonstrated that FCS_{hm} was composed of GlcA, GalNAc and Fuc at a ratio of 1:1:1.3.

The fucosyl branches generated by mild acidic hydrolysis were analyzed by HILIC-FTMS/MS. The extracted ion chromatograms are shown as Fig. 1, which demonstrated that fucooligosaccharides from degree of polymerization (dp) 1 to dp 5 with different sulfate patterns were existed in FCS_{hm}. Owing to desulfation and low contents, oligosaccharide ions with high sulfation and high degree of polymerization were difficult to analyze involved in ESI-CID-MS/MS. So fucosyl branches of dp1 to dp3 with a single sulfate group were selected as the precursor ion for CID-MS/MS analysis. According to the literature reported, the existence of $^{0,2}A$ and $^{0,3}A$ indicated the glycosidic linkage of fucose was α(1–4)-type (Anastyuk et al., 2010; Jin, Guo, Wang, Zhang, & Zhang, 2013), while $^{1,4}A$ unambiguously indicated α(1–3)-linked (Wu et al., 2015). The abundant $^{1,4}A_2$ ion at *m/z* 315 in Fig. S4B and two consecutive $^{1,4}A$-ions in Fig. S4C ($^{1,4}A_2$ at *m/z* 315 and $^{1,4}A_3$ at *m/z* 461) unambiguously indicated that both of the glycosidic bonds were α1,3-linked.

After mild acidic hydrolysis and chondroitin ABC digestion of acid-resistant fragments, FCS_{hm} displayed four sharp peaks of ΔUAβ1 → 3GalNAc (ΔDi-0S), ΔUAβ1 → 3GalNAc6S (ΔDi-6S), ΔUAβ1 → 3GalNAc4S (ΔDi-4S) and ΔUAβ1 → 3GalNAc4S6S (ΔDi-4,6S), respectively (Fig. 2). Percent distributions of disaccharide composition for FCS_{hm} were listed in Table S1, which meant the backbone of FCS_{hm} was mainly composed of chondrontin sulfate A (CSA) and chondrontin sulfate E (CSE).

3.2. NMR spectra analysis of FCS_{hm}

The structural features of FCS_{hm} were properly characterized through a combination of one-dimensional ^1H NMR, DEPTQ NMR, and two-dimensional ^1H–^1H COSY, ^1H–^1H NOESY, ^1H–^1H TOCSY, ^1H–^{13}C HSQC, ^1H–^{13}C HMBC spectra. Major ^1H and ^{13}C-chemical shifts (ppm) identified from these spectra have been listed in Table 1.

The ^1H NMR spectrum of FCS_{hm} had a crowded region between 3.4 and 5.0 ppm, resulting in a severe signal overlap for the majority of the resonances. In ^1H NMR spectrum, four notable anomeric proton signals between 5.0–6.0 ppm was consistent with H-1 of α-linked Fuc with different sulfate patterns: the signals at δ5.66, 5.39, 5.26, 5.32 ppm were assigned to 2,4-disulfated (FI), 4-sulfated (FII), 4-sulfated (FIII) and 3,4-sulfated (FIV) fucose respectively, in accordance with the low field shifts of C-2 (δ 80.11 ppm) and C-4 (δ 84.00 ppm) for FI, C-4 (δ 82.31 ppm) for FII, C-4 (δ 79.57 ppm) for FIII (Fig. 3A), whereas the low content of FIV resulted in extremely low signals in 2D spectra. The ratio of units FI: FII: FIII: FIV equal to 3:4:4:1 was determined in terms of the integral intensities of the respective H-1 in the ^1H NMR spectrum.

The anomeric carbons were deduced by DEPTQ NMR and 2D ^1H–^{13}C HSQC (Fig. 3B and E). Two characteristic β-anomeric $^1H/^{13}C$-signals at 4.48/106.11 and 4.64/102.40 ppm were respectively attributed to residues of GlcA (U1) and GalNAc (A1), while 5.66/99.22, 5.39/101.16, 5.26/100.63 and 5.32/101.51 ppm were consistent with FI1, FII1, FIII1 and FIV1. In addition, the signal at 4.29/70.09 ppm was ascribed to 6-sulfated GalNAc (A6(S)) units, whereas the signal was ~0.5 ppm shifted to high field in the ^1H-scale and ~6 ppm in the ^{13}C-scale (A6(US)) assigned to non-sulfated GalNAc residues.

In the ^1H–^{13}C HMBC spectrum, two clear signals involved in glycosydic bonds were at 3.98/102.40 and 3.67/106.11 ppm (denoted U4/A1 and A3/U1, respectively, in Fig. S5), which demonstrated β-(1–4) and β-(1–3) linkage type in chain backbone. As was the case of U3/FI1 and U3/FII1, it demonstrated α-(1–3) linkage type between Fuc and GlcA. The attachment of FI and FII to *O*-3 of GlcA was also confirmed by the data of ^1H–^1H NOESY (Fig. 3D). Such fucosyl branches were observed previously in FCS from *H. Mexicana* (Mou, Wang, Li, & Yang, 2017) and from other sea cucumber species. While particularly, FIII was linked to *O*-6 of GalNAc according to the correlation FIII1/A6 in ^1H–^1H NOESY and A6/FIII1 in ^1H–^{13}C HMBC, respectively (Figs. 3 D and S5). The low field shift of H-6 (δ4.15 ppm) for non-sulfated GalNAc indicated the formation of glucosidic bond between FIII and GalNAc. This fucosyl linkage type is rarely reported. Unfortunately, the signals among fucosyl branches were too weak to identify.

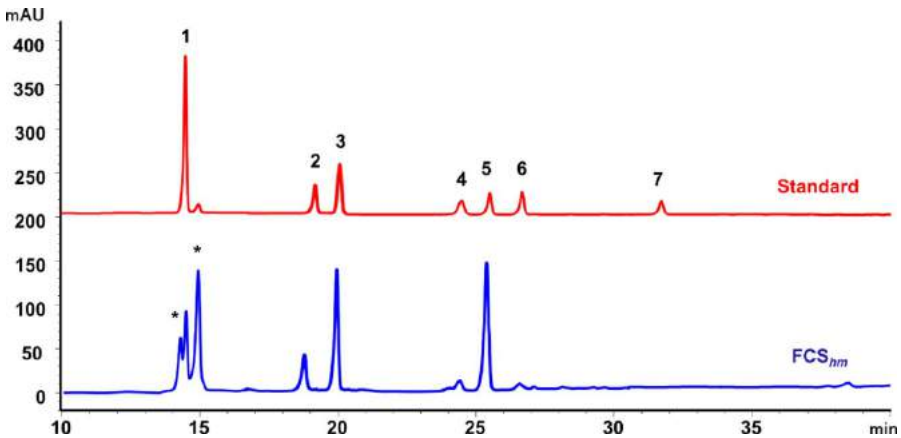

Fig. 2. HPLC chromatography of unsaturated disaccharide composition of FCS_{hm} after partial acidic hydrolysis. Disaccharides generated from exhaustive action of chondroitin ABC lyase on acid-resistant fragments of FCS_{hm} were tested. The red line represents seven disaccharide standards. Numbered peaks correspond to known disaccharide standards as follows: 1, ΔDi-0S; 2, ΔDi-6S; 3, ΔDi-4S; 4, ΔDi-2,6S; 5, ΔDi-4,6S; 6, ΔDi-2,4S; 7, ΔDi-2,4,6S; (ΔDi stands for ΔUAβ1 → 3GalNAc). Peaks labeled with "*" were contaminants from the reaction system. (For interpretation of the references to colour in this figure legend, the reader is referred to the web version of this article.)

Table 1
^{1}H and ^{13}C chemical shifts of FCS_{hm}.

Residue	GlcA (U)	GalNAc (A)	Fuc2,4S (FI)	Fuc4S (FII)	Fuc4S(FIII)	Fuc3S4S(FIV)
H1/C1	4.48/106.11	4.64/102.40	5.66/99.22	5.39/101.16	5.26/100.63	5.32/101.51
H2/C2	3.60/76.28	4.06/54.14	4.49/79.82	4.18/74.71	4.28/73.72	–
H3/C3	3.71/79.85	3.99/74.50	4.11/69.60	4.70/77.89	3.99/70.11	–
H4/C4	3.99/78.17	4.54/80.20	4.80/83.87	5.05/82.31	4.85/79.41	–
H5/C5	3.68/76.31	4.26/73.56	4.88/68.89	4.53/71.73	4.38/70.34	–
H6/C6	–/177.46	4.29/70.09(S) 3.78, 4.15/63.92(US)	1.34/18.47	1.34/18.47	1.34/18.47	–
C=O	–	-/177.46	–	–	–	–
CH_3	–	2.05/25.35	–	–	–	–

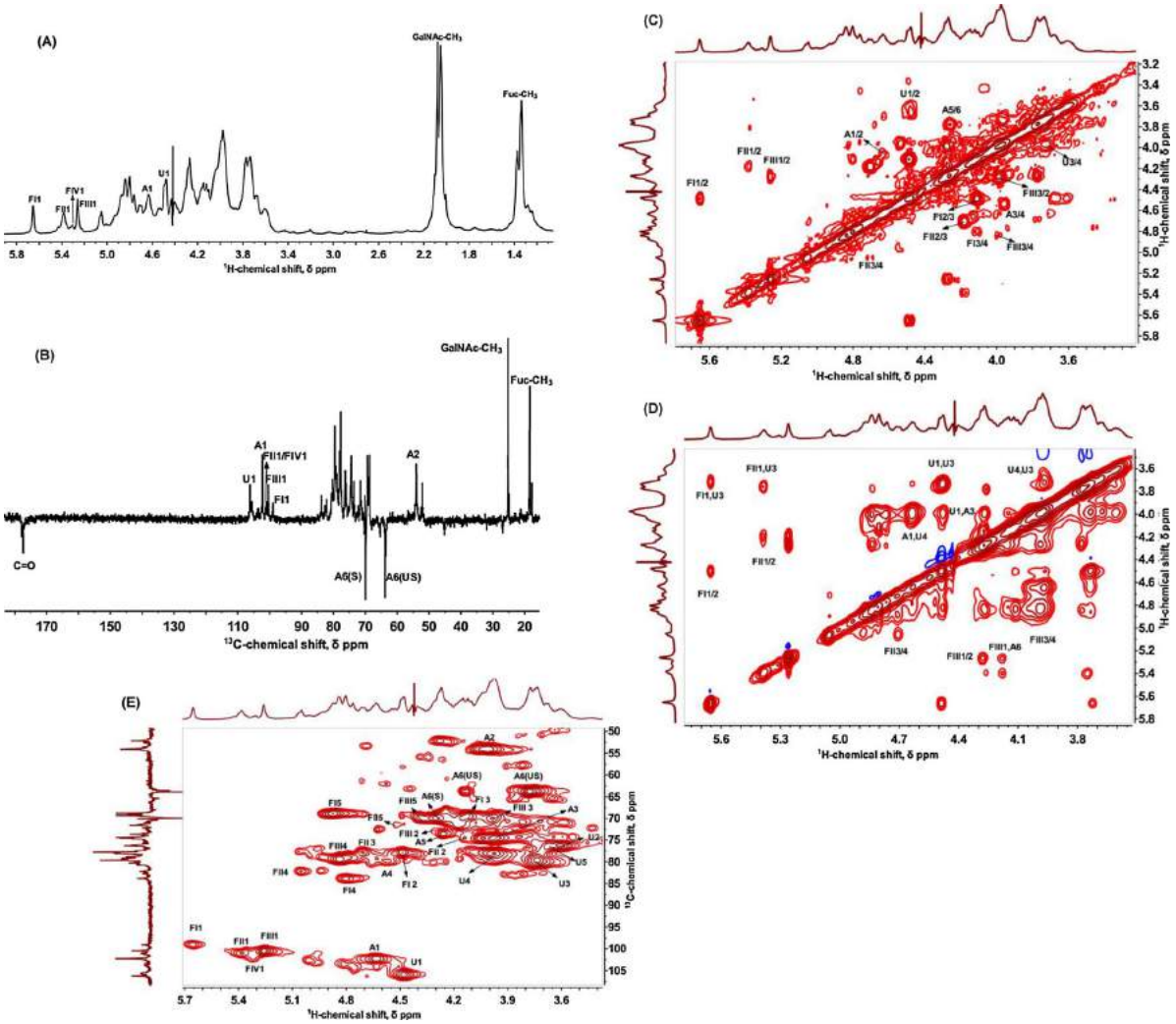

Fig. 3. 1D and 2D-NMR spectra of isolated FCS_{hm}: ^{1}H NMR(A), DEPTQ NMR (B) ^{1}H–^{1}H COSY (C), ^{1}H–^{1}H NOESY (D), ^{1}H–^{13}C HSQC (E). U, A, FI, FII, FIII and FIV stand for GlcA, GalNAc, Fuc-2S4S, Fuc-4S, Fuc-4S (attached to *O*-6 of GalNAc) and Fuc-3S4S (attached to *O*-6 of GalNAc), respectively.

3.3. HILIC-FTMS analysis of FCS_{hm}

The side chains of FCS_{hm} had been illuminated by mild acidic hydrolysis, and then the detailed structure was determined by HILIC-FTMS after free radical depolymerization. The total ion chromatogram of FCS_{hm} oligosaccharides based on HILIC-FTMS was shown as Fig. 4A. The raw data was deconvoluted using Decon Tools, and then, the output of Decon Tools was processed by GlycResoft to generate matching structures and provide relative quantitative information according to the ion abundance normalization (Li et al., 2014; Maxwell et al., 2012). Relative quantitative results of the major oligosaccharides were shown in Fig. 4B, and the existence of Fuc-GalNAc-aSO_3 (a = 0, 1, 2, 3) demonstrated FIV was also linked to GalNAc by α-(1–6) glucosidic bond, which were resistant with NMR and further proved approximately 42% of Fuc was directly linked to GalNAc.

The schematic diagram of the chemical structure of FCS_{hm} is shown as Fig. 5. Two branches, α-L-Fuc-2*S*4*S* and α-L-Fuc-4S were linked to *O*-3 of GlcA residue (FI and FII in Fig. 5), while others were identified as

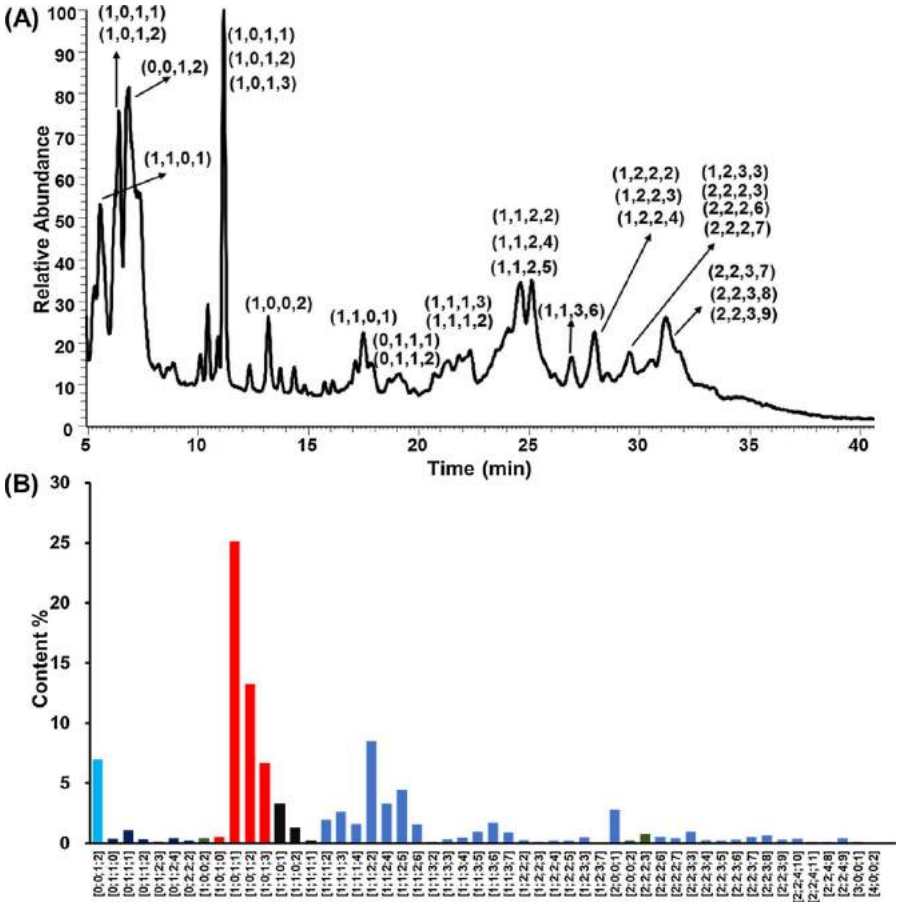

Fig. 4. HILIC-FTMS profiling of FCS_{hm} oligosaccharides generated by free radical depolymerization. (A) Total ion chromatography of FCS_{hm} oligosaccharides; (B) Composition analysis of FCS_{hm} oligosaccharides calculated by GlycResoft. The analytical error for each oligosaccharide was < 5%. Oligomer composition was given as [Fuc, GlcA, GalNAc, SO_3].

α-L-Fuc-4S and α-L-Fuc-3S4S attached to *O*-6 of GalNAc residue (FIII and FIV in Fig. 5). Additionally, a minority of FI, FII and FIII were α1,3-linked to other fucooligosaccharides from dp1 to dp4.

3.4. Fibroblast growth factor binding activities of FCS_{hm}

FGF1, a modifier of endothelial cell migration and proliferation, as well as an angiogenic factor, plays significant roles in angiogenesis and tumorigenesis (Relf et al., 1997). FGF2, also known as basic fibroblast growth factor, is present in basement membranes and subendothelial extracellular matrix of blood vessels in normal tissues. During both wound healing of normal tissues and tumor development, activated FGF2 mediates the formation of new blood vessels (Bhora et al., 1995; Katoh, 2008). J. Tapon et al. reported FCS extracted from the sea

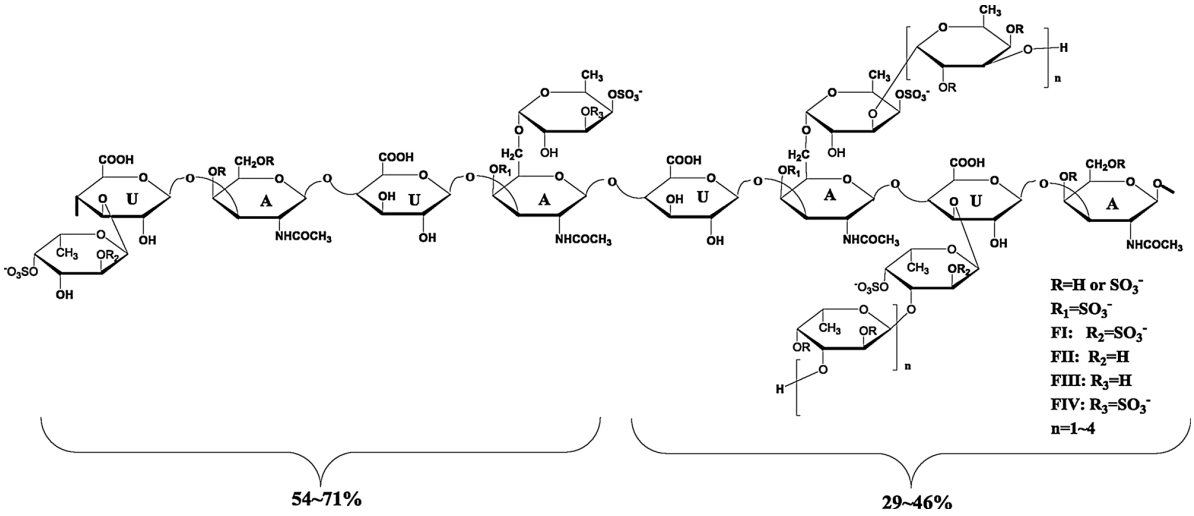

Fig. 5. Schematic diagram of the chemical structure of FCS_{hm}.

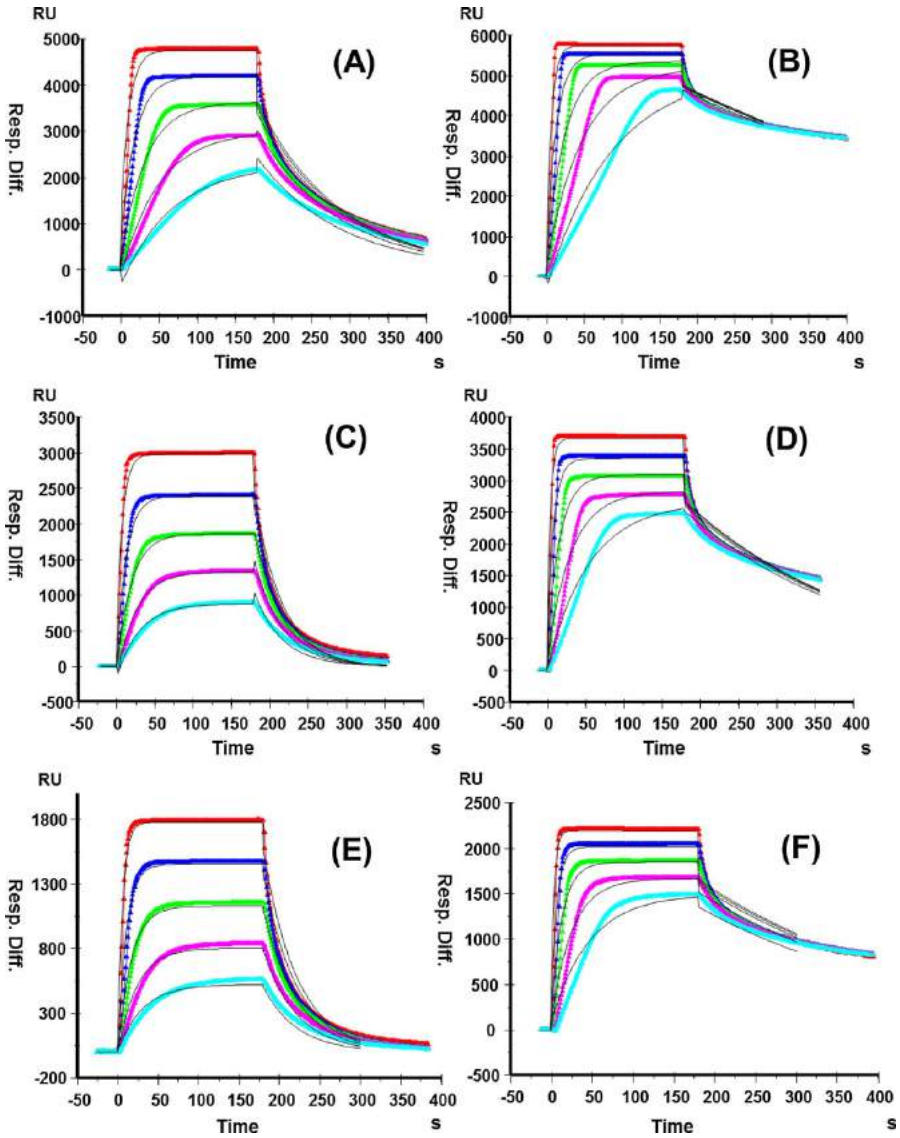

Fig. 6. SPR sensorgrams for interactions of FCS_{hm} with FGF1 and FGF2. Top row: commercial heparin (HP) bound to: (A) FGF1; (B) FGF2; Middle row: isolated FCS_{hm} bound to: (C) FGF1; (D) FGF2; Bottom row: isolated FCS-*Ib* bound to: (E) FGF1; (F) FGF2. The concentrations of each protein (from top to bottom): 1000, 500, 250, 125 and 63 nM, respectively. The black curves are the fitting curves using models from BIAevaluate 4.0.1.

cucumber *Ludwigothurea grisea* enhanced FGF-1 and FGF-2 induced HUVEC proliferation and selectively enhanced FGF-1 induced HUVEC migration (Taponbretaudière et al., 2000). However, no studies have shown the interaction between FCS and FGF in vitro.

SPR, a highly sensitive analytical technique that was used to measure the strength of molecular binding interactions, showed for the first time that FCS_{hm} exhibited strong binding abilities to FGF1 and FGF2 that was similar to heparin (Table S2 and Fig. 6). Thus, the strong binding abilities to FGF1 and FGF2 of the novel FCS_{hm} suggested that FCS_{hm} might improve angiogenesis as a potential therapeutic agent. In addition, to investigate the roles that fucosyl branch types play for the activity, we also determined the binding ability of FCS from *Isostichopus badionotus* (FCS-*Ib*). FCS-*Ib* contained a CSE backbone and 2,4-*O*-sulfated fucosyl branch, and the fucosyl branch of FCS-*Ib* was totally α(1,3)-linked to GlcA (Chen et al., 2011; Chen et al., 2013). The binding kinetics and affinity of FCS-*Ib* were listed at Table S2 and Fig. 6. FCS-*Ib* showed binding responses to FGF1 (K_D values of 1.63×10^{-7}) and FGF2 (K_D values of 1.32×10^{-8}), which was comparable to FCS_{hm} (K_D values of 2.74×10^{-7} and 1.89×10^{-8}, respectively). Therefore, it was inferred that the different linkage types of fucosyl branches hardly influence FGF binding ability of FCS. The strong binding ability may be attributed to the high anionic property that was similar to heparin.

3.5. Anticoagulant activities of FCS_{hm}

APTT is a performance indicator measuring the efficacy of intrinsic coagulation pathway and PT evaluates the extrinsic pathway of coagulation, while TT represents the common pathway of coagulation (Martinichen-Herrero, Carbonero, Gorin, & Iacomini, 2005). The anticoagulant activities of FCS_{hm} were evaluated using APTT, PT and TT of plasma clotting assays in comparison with low molecular weight heparin (LMWH). As the results of significant prolongation of APTT and TT (Fig. 7A and B), FCS_{hm} displayed intrinsic anticoagulant activity similar to LMWH and barely affected PT. However, the anticoagulant activity of FCS_{hm} was weaker than FCS-*Ib* that similarly to heparin (Chen et al., 2011; Chen et al., 2013). It was due to the higher sulfation degree of fucosyl branches in FCS-*Ib* than that in FCS_{hm}. And standards of CSA, CSC and CSE exhibited no anticoagulant activity, which indicated the sulfated α-fucosyl branches were essential for anticoagulation. In addition, APTT activities of FCS_{hm} showed a dose-

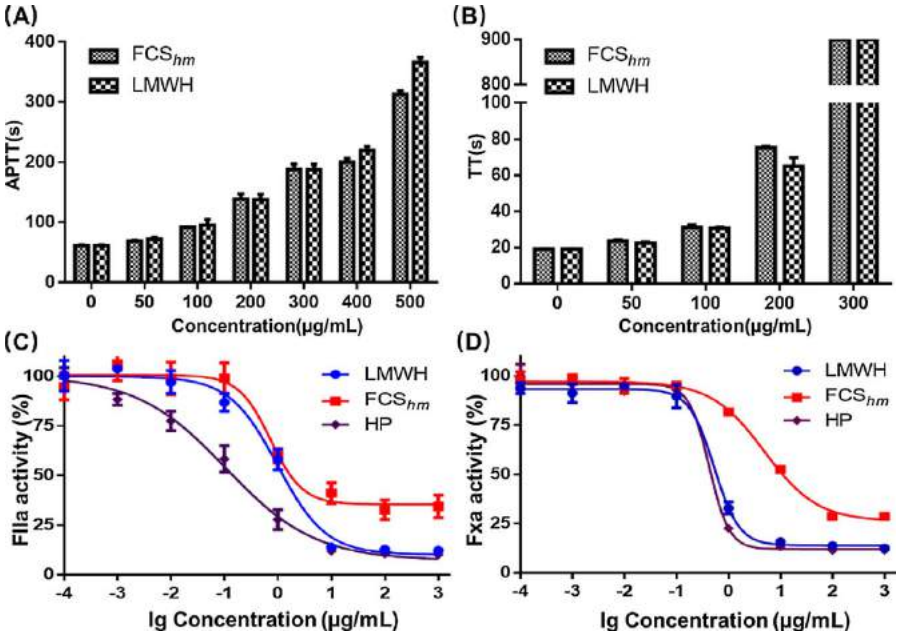

Fig. 7. The anticoagulant activities of FCS$_{hm}$. Effect of FCS$_{hm}$ and LMWH on prolong of the APTT (A) and TT (B). Effects of FCS$_{hm}$ on inhibition of FIIa (C) and FXa (D) by ATIII.

dependent inhibitory manner, while TT inhibitory activities of FCS$_{hm}$ increased sharply when the concentration was over 200 μg/mL. Furthermore, FCS$_{hm}$ exhibited strong ATIII-dependent anti-FIIa and anti-FXa activities (Fig. 7C and D). FIIa and FXa were associated with coagulation and thrombosis. Through high binding affinity to ATIII, FCS$_{hm}$ inhibited the activities of FIIa and FXa to achieve anticoagulant and antithrombotic effect. Hence FCS$_{hm}$ could be used as a potential replacement of LMWH and a potential agent to improve thrombosis.

In our previous studies, we isolated two FCS from *Cucumaria frondosa* and *Thelenota ananas*, and proved their potential effect in treatment of cancer and cancer-associated thrombosis (Liu, Hao et al., 2016; Liu, Liu et al., 2016). Based on the potential application prospects in anti-angiogenesis and antithrombosis, it was indicated that FCS$_{hm}$ also had the potential to treat cancer and cancer-associated thrombosis.

4. Conclusion

In this study, a novel structure of FCS (FCS$_{hm}$) was isolated from sea cucumber *H. Mexicana*. Structural analysis was determined by multi-dimensional NMR spectra and HILIC-FTMS, and we demonstrated the backbone of FCS$_{hm}$ was composed of CSA and CSE. Moreover, four types of branches were found in FCS$_{hm}$ with the ratio of 3:4:4:1. Two branches were α-L-Fuc-2S4S and α-L-Fuc-4S linked to *O*-3 of GlcA residue, while others were identified as α-L-Fuc-4S and α-L-Fuc-3S4S attached to *O*-6 of GalNAc residue. Furthermore, the fucosyl branches were consisted of dp1 to dp5 oligosaccharides in α-1,3-linkage type. Additionally, FCS$_{hm}$ was proven to have remarkable binding affinities to FGF1 and FGF2, growth factors involved in promoting endothelial cell migration, smooth muscle cell proliferation and neovascularization. And it had been proved the different linkage types of fucosyl branches hardly influence FGF binding ability of FCS. Moreover, FCS$_{hm}$ displayed intrinsic anticoagulant activity similar to LMWH and inhibited FIIa and FXa activities by ATIII. Our results proposed a novel structural fucosylated chondroitin sulfate and demonstrated its favorable application prospects in anti-angiogenesis and anticoagulation.

Acknowledgements

This work was supported by Grants from NSFC-Shandong Joint Fund for Marine Science Research Centers (U1606403), National Natural Science Foundation of China (31670811, 31600646), Major Science and Technology projects in Shandong province (2015ZDJS04002), China Postdoctoral Science Foundation funded project (2015M580610, 2016T90654), the Fundamental Research Funds for the Central Universities (201762002), the Scientific and Technological Innovation Project Financially Supported by Qingdao National Laboratory for Marine Science and Technology (2015ASKJ02) and Taishan scholar project special funds.

Appendix A. Supplementary data

Supplementary data associated with this article can be found, in the online version, at http://dx.doi.org/10.1016/j.carbpol.2017.10.100.

References

Anastyuk, S. D., Shevchenko, N. M., Nazarenko, E. L., Imbs, T. I., Gorbach, V. I., Dmitrenok, P. S., et al. (2010). Structural analysis of a highly sulfated fucan from the brown alga Laminaria cichorioides by tandem MALDI and ESI mass spectrometry. *Carbohydrate Research, 345*, 2206–2212.

Bhora, F. Y., Dunkin, B. J., Batzri, S., Aly, H. M., Bass, B. L., Sidawy, A. N., et al. (1995). Effect of growth factors on cell proliferation and epithelialization in human skin. *Journal of Surgical Research, 59*, 236–244.

Chen, S., Xu, J., Xue, C., Dong, P., Sheng, W., Yu, G., et al. (2008). Sequence determination of a non-sulfated glycosaminoglycan-like polysaccharide from melanin-free ink of the squid *Ommastrephes bartrami* by negative-ion electrospray tandem mass spectrometry and NMR spectroscopy. *Glycoconjugate Journal, 25*, 481–492.

Chen, S., Xue, C., Yin, L. A., Tang, Q., Yu, G., & Chai, W. (2011). Comparison of structures and anticoagulant activities of fucosylated chondroitin sulfates from different sea cucumbers. *Carbohydrate Polymers, 2*, 688–696.

Chen, S., Li, G., Wu, N., Guo, X., Liao, N., Ye, X., et al. (2013). Sulfation pattern of the fucose branch is important for the anticoagulant and antithrombotic activities of fucosylated chondroitin sulfates. *Biochimica et Biophysica Acta (BBA) – General Subjects, 1830*, 3054–3066.

Conand, C., & Byrne, M. (1993). A review of recent developments in the world sea cucumber fisheries. *Marine Fisheries Review, 55*, 1–13.

Conand, C. (2001). Overview of sea cucumbers fisheries over the last decade-what possibilities for a durable management. *Echinoderms 2000. Proceedings of the Tenth International Conference, Dunedin* (pp. 339–344).

Courjal, F., Cuny, M., Simony-Lafontaine, J., Louason, G., Speiser, P., Zeillinger, R., et al. (1997). Mapping of DNA amplifications at 15 chromosomal localizations in 1875 breast tumors: Definition of phenotypic groups. *Cancer Research, 57*, 4360–4367.

Deng, N., Liang, K. G., Wang, H., Das, K., Tao, J., Tan, I. B., et al. (2012). A comprehensive survey of genomic alterations in gastric cancer reveals systematic patterns of molecular exclusivity and co-occurrence among distinct therapeutic targets. *Gut, 61*,

673–684.
Dodgson, K. S., & Price, R. G. (1962). A note on the determination of the ester sulphate content of sulphated polysaccharides. *Biochemical Journal, 84*, 106–110.
Eswarakumar, V. P., Lax, I., & Schlessinger, J. (2005). Cellular signaling by fibroblast growth factor receptors. *Cytokine & Growth Factor Reviews, 16*, 139–149.
Hu, T., Huang, Q., Wong, K., & Yang, H. (2017). Structure, molecular conformation, and immunomodulatory activity of four polysaccharide fractions from *Lignosus rhinocerotis* sclerotia. *International Journal of Biological Macromolecules, 94*, 423–430.
Jin, W., Guo, Z., Wang, J., Zhang, W., & Zhang, Q. (2013). Structural analysis of sulfated fucan from Saccharina japonica by electrospray ionization tandem mass spectrometry. *Carbohydrate Research, 369*, 63–67.
Kariya, Y., Watabe, S., Hashimoto, K., & Yoshida, K. (1990). Occurrence of chondroitin sulfate E in glycosaminoglycan isolated from the body wall of sea cucumber *Stichopus japonicus*. *Journal of Biological Chemistry, 265*, 5081–5085.
Kariya, Y., Kyogashima, M. I. M., Ishii, T., & Watabe, S. (1997). Structure of fucose branches in the glycosaminoglycan from the body wall of the sea cucumber *Stichopus japonicus*. *Carbohydrate Research, 297*, 273–279.
Katoh, M. (2002). WNT and FGF gene clusters (review). *International Journal of Oncology, 21*, 1269–1273.
Katoh, M. (2008). Cancer genomics and genetics of FGFR2 (Review). *International Journal of Oncology, 33*, 233–238.
Lawrence, A. J. (2010). Bioactivity as an options value of sea cucumbers in the Egyptian Red Sea. *Conservation Biology, 24*, 217–225.
Li, G., Steppich, J., Wang, Z., Sun, Y., Xue, C., Linhardt, R. J., et al. (2014). Bottom-up low molecular weight heparin analysis using liquid chromatography-Fourier transform mass spectrometry for extensive characterization. *Analytical Chemistry, 86*, 6626–6632.
Lian, W., Wu, M., Huang, N., Gao, N., Xiao, C., Li, Z., et al. (2013). Anti-HIV-1 activity and structure-activity-relationship study of a fucosylated glycosaminoglycan from an echinoderm by targeting the conserved CD4 induced epitope. *Biochimica et Biophysica Acta (BBA)–General Subjects, 1830*, 4681–4691.
Liu, X., Hao, J., Shan, X., Zhang, X., Zhao, X., Li, Q., et al. (2016). Antithrombotic activities of fucosylated chondroitin sulfates and their depolymerized fragments from two sea cucumbers. *Carbohydrate Polymers, 152*, 343–350.
Liu, X., Liu, Y., Hao, J., Zhao, X., Lang, Y., Fan, F., et al. (2016). In vivo anti-cancer mechanism of low-molecular-weight fucosylated chondroitin sulfate (LFCS) from sea cucumber *Cucumaria frondosa*. *Molecules, 21*, 625.
Martinichen-Herrero, J. C., Carbonero, E. R., Gorin, P. A. J., & Iacomini, M. (2005). Anticoagulant and antithrombotic activity of a sulfate obtained from a glucan component of the lichen *Parmotrema mantiqueirense* Hale. *Carbohydrate Polymers, 60*, 7–13.
Maxwell, E., Tan, Y., Tan, Y., Hu, H., Benson, G., Aizikov, K., et al. (2012). GlycReSoft: A software package for automated recognition of glycans from LC/MS data. *PLoS One, 7*, e45474.
Mou, J., Wang, C., Li, W., & Yang, J. (2017). Purification, structural characterization and anticoagulant properties of fucosylated chondroitin sulfate isolated from *Holothuria mexicana*. *International Journal of Biological Macromolecules, 98*, 208–215.
Mourão, P. A., Pereira, M. S., Pavao, M. S., Mulloy, B., Tollefsen, D. M., Mowinckel, M. C., et al. (1996). Structure and anticoagulant activity of a fucosylated chondroitin sulfate from echinoderm. Sulfated fucose branches on the polysaccharide account for its high anticoagulant action. *Journal of Biological Chemistry, 271*, 23973–23984.
Mourão, P. A., Giumar Es, B., Mulloy, B., Thomas, S., & Gray, E. (1998). Antithrombotic activity of a fucosylated chondroitin sulphate from echinoderm: Sulphated fucose branches on the polysaccharide account for its antithrombotic action. *British Journal of Haematology, 101*, 647–652.
Mourão, P. A., Boissonvidal, C., Taponbretaudière, J., Drouet, B., Bros, A., & Fischer, A. (2001). Inactivation of thrombin by a fucosylated chondroitin sulfate from echinoderm. *Thrombosis Research, 102*, 167–176.
Pomin, V. H. (2014a). Holothurian fucosylated chondroitin sulfate. *Marine Drugs, 12*, 232–254.
Pomin, V. H. (2014b). How to analyze the anticoagulant and antithrombotic mechanisms of action in fucanome and galactanome? *Glycoconjugate Journal, 2*, 89–99.
Relf, M., LeJeune, S., Scott, P. A., Fox, S., Smith, K., Leek, R., et al. (1997). Expression of the angiogenic factors vascular endothelial cell growth factor, acidic and basic fibroblast growth factor, tumor growth factor beta-1, platelet-derived endothelial cell growth factor, placenta growth factor, and pleiotrophin in human primary breast cancer and its relation to angiogenesis. *Cancer Research, 57*, 963–969.
Taponbretaudière, J., Drouet, B., Matou, S., Mourão, P. A., Bros, A., Letourneur, D., et al. (2000). Modulation of vascular human endothelial and rat smooth muscle cell growth by a fucosylated chondroitin sulfate from echinoderm. *Thrombosis & Haemostasis, 84*, 332–337.
Taponbretaudière, J., Chabut, D., Zierer, M., Matou, S., Helley, D., Bros, A., et al. (2002). A fucosylated chondroitin sulfate from echinoderm modulates in vitro fibroblast growth factor 2-dependent angiogenesis. *Molecular Cancer Research, 1*, 96–102.
Turner, N., Lambros, M. B., Horlings, H. M., Pearson, A., Sharpe, R., Natrajan, R., et al. (2010). Integrative molecular profiling of triple negative breast cancers identifies amplicon drivers and potential therapeutic targets. *Oncogene, 29*, 2013–2023.
Ustyuzhanina, N. E., Bilan, M. I., Dmitrenok, A. S., Tsvetkova, E. A., Shashkov, A. S., Stonik, V. A., et al. (2016). Structural characterization of fucosylated chondroitin sulfates from sea cucumbers *Apostichopus japonicus* and *Actinopyga mauritiana*. *Carbohydrate Polymers, 153*, 399–405.
Ustyuzhanina, N. E., Bilan, M. I., Dmitrenok, A. S., Shashkov, A. S., Nifantiev, N. E., & Usov, A. I. (2017). The structure of a fucosylated chondroitin sulfate from the sea cucumber Cucumaria *frondosa*. *Carbohydrate Polymers, 165*, 7–12.
Vieira, R. P., Mulloy, B., & Mourão, P. A. (1991). Structure of a fucose-branched chondroitin sulfate from sea cucumber: Evidence for the presence of 3-*O*-sulfo-beta-D-glucuronosyl residues. *Journal of Biological Chemistry, 266*, 13530–13536.
Weiss, J., Sos, M. L., Seidel, D., Peifer, M., Zander, T., Heuckmann, J. M., et al. (2010). Frequent and focal FGFR1 amplification associates with therapeutically tractable FGFR1 dependency in squamous cell lung cancer. *Science Translational Medicine, 2*, 62r–93r.
Weyers, A., Yang, B., Solakyildirim, K., Yee, V., Li, L., Zhang, F., et al. (2013). Isolation of bovine corneal keratan sulfate and its growth factor and morphogen binding. *FEBS Journal, 280*, 2285–2293.
Wu, N., Ye, X., Guo, X., Liao, N., Yin, X., Hu, Y., et al. (2013). Depolymerization of fucosylated chondroitin sulfate from sea cucumber, Pearsonothuria graeffei, via 60Co irradiation. *Carbohydrate Polymers, 93*, 604–614.
Wu, J., Lv, Y., Liu, X., Zhao, X., Jiao, G., Tai, W., et al. (2015). Structural study of sulfated fuco-oligosaccharide branched glucuronomannan from kjellmaniella crassifolia by ESI-CID-MS/MS. *Journal of Carbohydrate Chemistry, 34*, 303–317.
Zhou, X., Xu, G., & Shen, B. (2008). Effect of freeze-dried sea cucumber powder of eastern sea on tumor and immune index of S180-bearing mouse. *Journal of Hygiene Research, 37*, 30–32.